Investigation of Artificial Intelligence Algorithms for MPPT of Solar Photovoltaic System

MOHAMED I. ABU EL-SEBAH[1], ALY M. EISSA[2], MOHAMED FAWZY EL-KHATIB[2]
[1]Power Electronics and Energy Conversion Department,
Electronics Research Institute,
Cairo 11843,
EGYPT

[2]Mechatronics and Robotics Engineering Department, Faculty of Engineering,
Egyptian Russian University,
Cairo 11829,
EGYPT

Abstract:- Solar energy has gained prominence as a primary renewable energy source for the generation of electricity in recent years. The maximization of power extraction from photovoltaic (PV) systems is a topic of significant interest due to the relatively low conversion efficiency of these systems. Therefore, a maximum power point tracking (MPPT) controller is essential in a PV system to achieve the desired output power. This paper implements three different MPPT controllers: sliding mode control (SMC), fuzzy logic controller (FLC), and artificial neural networks (ANNs). The performance of these controllers is evaluated on a PV system under varying irradiation and temperature conditions to analyze their ability to track the maximum power point (MPP). The results demonstrate that the SMC outperforms the FLC and ANN in terms of best performance with minimum oscillation under different operating conditions.

Key-Words:- Photovoltaic system, Boost converter, Sliding mode control, Artificial Neural Networks, Fuzzy Logic Controller, Simulation.

Received: March 19, 2023. Revised: December 4, 2023. Accepted: December 21, 2023. Published: December 31, 2023.

1 Introduction

In today's world, there is a growing need, for energy sources, like power, wind energy, and biomass to meet the increasing electricity needs of consumers. These sources are pristine, abundant, and pollution-free. Photovoltaic (PV) is a prominent clean energy source that efficiently powers electrical loads and may also feed energy back into the utility system. MPP operation is necessary because of the nonlinearity of the PV system's output. To ensure the continuous operation of MPP under varying ambient temperatures and solar radiation conditions, the use of control algorithms is necessary. It is difficult to determine which MPP has the smallest oscillation in proximity to the operational point, [1], [2], [3], [4].

Two ways to follow the MPP, the first is the conventional methods such as Fractional open circuit (OC) voltage, Fractional short circuit (SC) current, Incremental conductance (IC), and Perturbation and observation (P&O). The main limitation of most of these earlier algorithms is their tendency to oscillate in the vicinity of the operating point in a steady state. Additionally, the direction of tracking the MPP is disrupted due to swiftly changing atmospheric conditions, [5], [6], [7], [8], [9].

The second is the intelligence methods such as FLC and ANN, SMC, and others. The ANN method must have undergone training using a significant number of solar irradiance and ambient temperature measurements. The FLC is sensitive to voltage variations and the current output from the PV panel. The system utilizes the derivative of power concerning current (dP/dI) and its derivatives as the inputs and calculates the duty cycle of the MPPT converter, [10], [11], [12], [13]. The SMC uses a step size that can be adjusted on the fly. When the operational point is significantly distant from the sliding surface, this method increases the step size to expedite progress. Given that the effective point is near the sliding surface, the system will experience smaller step sizes, resulting in a shortened duration of oscillation around the maximum power point (MPP), [14], [15], [16], [17], [18]. The novelty can be summarized as:

1. Developing and adapting the FLC, ANN, and SMC based MPPT to optimize the power output of a PV with a resistive load.
2. Tracking of the MPP under different operating conditions during constant irradiance levels, rapid changes in irradiance levels, and rapid changes in temperature levels.

The organization of this paper will be as follows: Section 2 introduces the photovoltaic system. Section 3 describes the boost converter design. Sections 4, 5, and 6 present the MPPT controllers: SMC, FLC, and ANN, respectively. Section 7 shows the simulation results, while Section 8 presents the conclusion.

2 Photovoltaic System

The solar system under consideration, seen in Fig. 1, employs the PV system, whose electrical properties are listed in Table 1, a boost converter, a neural network based MPPT controller, and a resistive load, [19], [20], [21], [22], [23].

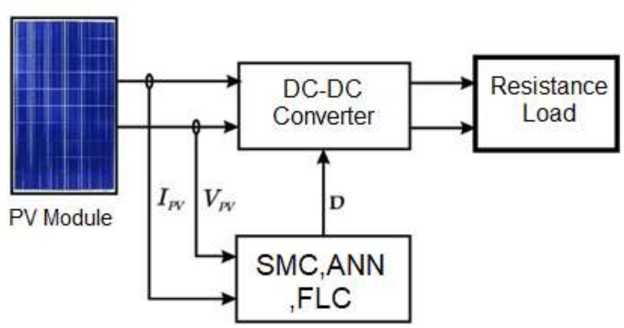

Fig. 1: Block diagram of the proposed system

Table 1. Parameters of PV module.

Module Characteristics	Values
P_{max}	220 W
V_{max}	30 V
I_{max}	7.35 A
I_{SC}	8.81 A
V_{OC}	36.8V

The single-diode variant strikes a good balance between ease of use and precision. In Figure 2, we see a photocurrent source connected in parallel with a nonlinear diode, a shunt resistor, and a series resistor. The photocurrent's origin is largely established by the cell's operational temperature and the amount of solar irradiation it receives. These equations characterize the PV cell model, [24], [25], [26]:

$$I = I_{ph} - I_D - I_{sh} \tag{1}$$

$$I = I_{ph} - I_S\left[exp(\frac{q(V+IR_S)}{K_C A}) - 1\right] - \frac{V+IR_s}{R_{sh}} \tag{2}$$

$$I_{ph} = [I_{SC} + K_1(T_C - T_r)]\lambda \tag{3}$$

Where I_{ph}: photocurrent current, I_D: diode current, I: output current from the cell, I_{Sh}: shunt resistor current, I_S: saturation current of the diode, K_1: Boltzmann constant, q: electron charge, T_c: actual temperature of the cell, R_{Sh}: shunt resistance, and I_{SC}: short-circuit current, T_r: reference temperature, λ: irradiance and R_{Sh}: series resistance, V and I are the output current and voltage of the PV module respectively.

3 Boost Converter Design

The following clause describes the modeling of the dynamic behavior of the boost converter, [27], [28], [29], [30]:

When the switch is on:

$$V_{pv} = V_L = L\frac{di_L}{dt} \tag{4}$$

When the switch is off:

$$V_{pv} = V_L + V_o = L\frac{di_L}{dt} + V_o \tag{5}$$

The dynamic characteristics of the boost converter are from (6) and (7):

$$\frac{di_L}{dt} = \frac{V_{pv} - V_o(1-u)}{L} \tag{6}$$

Where V_{pv}: is the PV array voltage, i_L: the inductor current V_o: the converter output voltage, and V_L: is the converter inductor voltage.

4 Sliding Mode Control

SMC is a type of dynamic controller that is used to create resilient controllers for complicated, high-order, nonlinear dynamic plants that operate in uncertain settings. There are two fundamental concepts underlying SMC, the first creating a sliding surface that will function as the operational point in the initial stage. Secondly, within a finite amount of time, establishing a control law that shifts the effective point to a predetermined surface, [31], [32], [33], [34].

Begin by developing a surface within state space.

- The process of choosing a control law that compels the system's state path to approach a pre-established surface within a limited period.
- Sustaining it in proximity to this surface by employing suitable switching logic.

The SMC dynamic analysis: sliding surface proposition to be:

$$S = \left(V_{pv} - V_{ref}\right) \cdot G_1 + i_{Cin} \cdot G_2 \tag{7}$$

with G1 and G2 representing constant gains.

To implement the suggested method, (S) must equal zero and dS must be:

$$\frac{dS}{dt} = \left(\frac{dV_{pv}}{dt} - \frac{dV_{\text{ref}}}{dt}\right) \cdot G_1 + \frac{di_{\text{Cin}}}{dt} \cdot G_2 \tag{8}$$

$$i_{Cin} = i_{pv} - i_L \tag{9}$$

$$i_{\text{Cin}} = C_{in} \frac{dV_{\text{Cin}}}{dt} \tag{10}$$

from (9) and (10) we obtain the following equation

$$\frac{dV_{pv}}{dt} = \frac{i_{pv} - i_L}{C_{in}} \tag{11}$$

Substituting (9) and (10) in (6)

$$\frac{dS}{dt} = \left(\frac{i_{pv} - i_L}{C_{in}} - \frac{dV_{ref}}{dt}\right) \cdot G_1 + \left(\frac{di_{pv}}{dt} - \frac{di_L}{dt}\right) \cdot G_2 \tag{12}$$

Substituting (3) in (6)

$$\frac{dS}{dt} = \left(\frac{i_{pv} - i_L}{C_{in}} - \frac{dV_{ref}}{dt}\right) \cdot G_1 + \left(\frac{di_{pv}}{dt} - \frac{V_{pv}}{L} + \frac{V_o(1-u)}{L}\right) \cdot G_2 = 0 \tag{13}$$

Equation (7) thus characterizes the SMC dynamic model, in which the successful implementation of the proposed method is ensured by the optimization of the fixed gains and parameters for the boost converter.

5 Fuzzy Logic Control

By regulating the duty cycle of the converter, the FLC targets to optimize the monitoring efficiency of the MPP of the PV panel. The inputs of the FLC correspond to the PV panel output current and voltage, whereas the output of the controller signifies the duty cycle. To optimize power output, the FLC controls the voltage through the converter duty ratio, which is determined by the power ratio (dp/dv) change. The FLC is utilized to regulate the DC converter and accepts duty cycle (CD), error (E), and change in error (CE) signals as inputs. The parameters for the input and output are as follows, [35], [36], [37]:

$$E(k) = \frac{P(k) - P(k-1)}{V(k) - V(k-1)} \tag{14}$$

$$CE(k) = E(k) - E(k-1) \tag{15}$$

$$CD = f(E, CE) \tag{16}$$

Where the immediate power (P(k)) and instant voltage (V(k)) of the PV are denoted as such.

The direction in which the load target point at instant k is moving is denoted by the change in error, while the input error E(k) shows whether the target point of the load is to the right or left of the MPP of the PV panel. The controller's design comprises three fundamental components: defuzzification, base rule, and fuzzification, [38], [39], [40], [41], [42]. The input and output membership functions of the controller are illustrated in Figure 2. The FLC rule includes 25 rules, as described in Table 2.

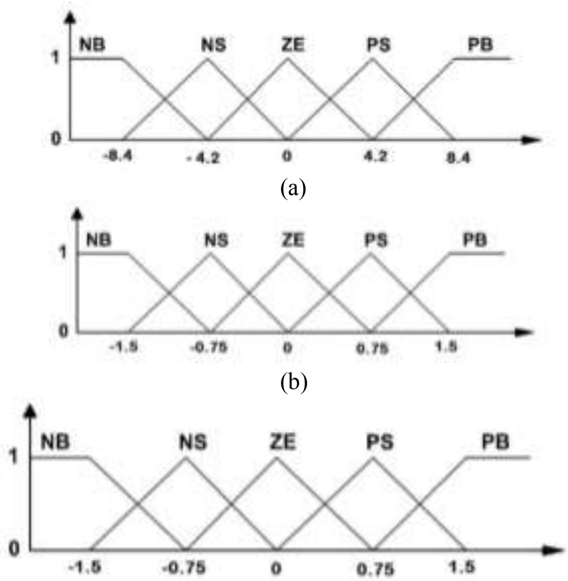

(c)
Fig. 2: Fuzzy system membership function. (a) E. (b) CE. (c) CD

Table 2. Rules of the FLC

E	CE				
	NB	NS	ZE	PS	PB
NB	PS	PB	NB	NB	NS
NS	PS	PS	NS	NS	NS
ZE	ZE	ZE	ZE	ZE	ZE
PS	NS	NS	PS	PS	PS
PB	NS	NB	PB	PB	PS

6 Artificial Neural Network

There are several ways in which AI methods excel over more conventional methods. Traditional systems have limitations including being slow to adapt to shifting solar temperature and irradiance, and occasionally failing to keep tabs on the peak power point. Input data (such as irradiance and temperature) is received by the input layer, and from there is sent to the second and third layers via a network of hidden neurons. The converter's output (duty cycle) is supplied by the third layer. To determine the MPP, a three-layer neural network is illustrated in Figure 3. The input layer is responsible for receiving input data, which consists of temperature and irradiation. Several concealed neurons are located in hidden layers, from which the input layer transmits data to the third layer. The duty ratio output is supplied to the converter by the third layer. The inputs and outputs are, [43], [44], [45], [46], [47]:

$$Y_j^h = f\left(\sum_{i=1}^{N} W_{ij} X_i + \theta_j^h\right) \quad (17)$$

$$Y_k^o = f\left(\sum_{j=1}^{N} W_{kj} Y_j^h + \theta_k^o\right) \quad (18)$$

Where W_{ij} and W_{kj}: The lines linking the three levels are allocated weights; θ_k^o and θ_j^h: The bias values associated with the concealed layer and output, respectively; X_i and Y_j^h: The signal values about the input and output lines.

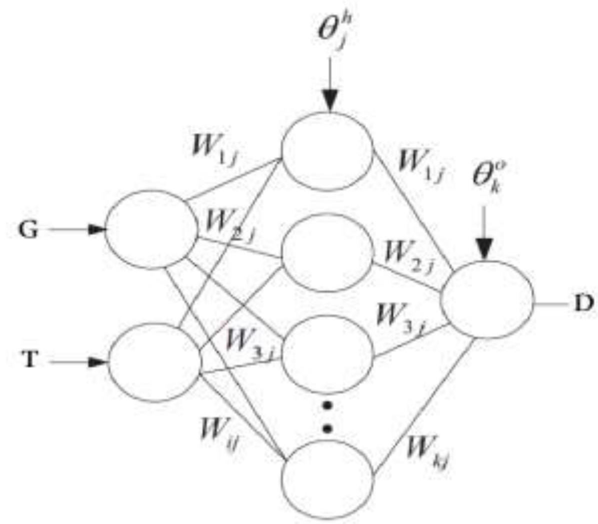

Fig. 3: The construction of the ANN

7 Results and Discussion

The simulations utilized in this research were carried out through the implementation of systems in MATLAB, which execute the suggested SMC, ANN, and FLC. The output PV power of the SMC, FLC, and ANN using constant conditions (T = 25C, G = 1000W/m^2) is depicted in Figure 4. The SMC exhibits superior characteristics in terms of rise time, response time, and absence of overshoot when compared to the ANN and FLC, [48], [49], [50], [51], [52], [53].

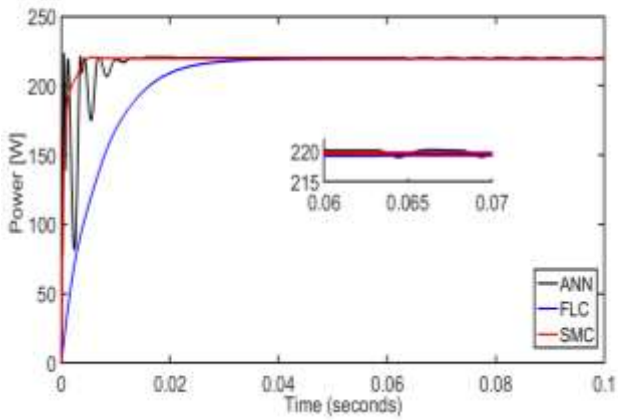

Fig. 4: An analysis of the three controllers in comparison to a constant atmospheric condition

For the three controllers, Figure 5 depicts the PV output power when the irradiance drops abruptly from 1000 W/m^2 to 800 W/m^2, then to 600 W/m^2, and ultimately to 400 W/m^2. They possess an exceptional capacity to monitor the MPP by the four controllers. However, the rise and settling periods of the SMC are shorter.

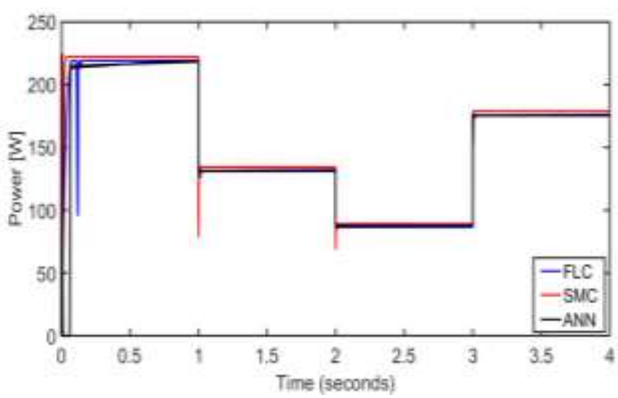

Fig. 5: The power output of the three controllers at a constant 25 C and varying levels of irradiance.

The PV output power for all three controllers is depicted in Figure 6, with temperature fluctuations and irradiance of 1000 W/m^2 held constant. The temperature fluctuated between 25C and 30C, then 35C, 40C, and 25C once more. It is noteworthy that they possess an exceptional capability to monitor the MPP for every controller. However, the rise and settling periods of the SMC are shorter.

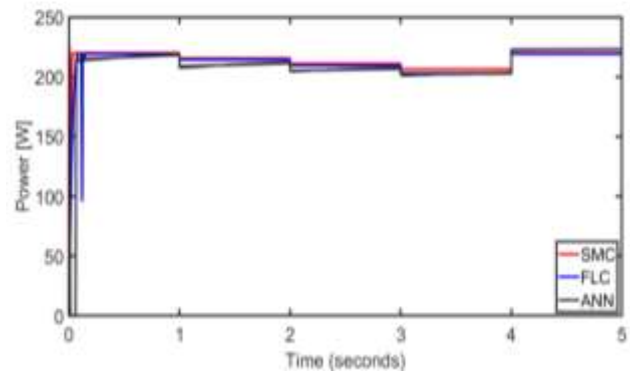

Fig. 6: The power output of the three controllers as the temperature and irradiance levels remain constant.

8 Conclusions

This paper describes various MPPT control algorithms utilized to determine the MPP of a PV panel subjected to variable conditions. The SMC, FLC, and ANN were devised to monitor the MPP across diverse atmospheric conditions. To assess the effectiveness of the controllers being evaluated, a variety of scenarios were investigated. These scenarios comprised consistent irradiance levels, precipitous fluctuations in irradiance levels, and abrupt temperature changes. In contrast to FLC and SMC, the results demonstrate that the SMC can monitor the reference rapidly and with superior performance. At a steady condition, the MPP is devoid of any oscillation.

References:

[1] El-Khatib, M. F., Sabry, M. N., El-Sebah, M. I. A., & Maged, S. A. (2023). Hardware-in-the-loop testing of simple and intelligent MPPT control algorithm for an electric vehicle charging power by photovoltaic system. *ISA transactions*, *137*, 656-669.

[2] Mohamed Fawzy El-Khatib, Elsayed Atif Aner. Efficient MPPT control for a photovoltaic system using artificial neural networks. *ERU Research Journal*, 2023, 1-14.

[3] Kraiem, H., Flah, A., Mohamed, N., Alowaidi, M., Bajaj, M., Mishra, S., & Sharma, S. K. (2021). Increasing electric vehicle autonomy using a photovoltaic system controlled by particle swarm optimization. *IEEE Access*, 9, 72040-72054.

[4] Das P. Maximum power tracking based open circuit voltage method for PV system. *In:*

International Conference on Advances in Energy Research (ICAER), Mumbai, India, 15–17 December 2015 published by Elsevier. p. 2–13.

[5] Dil X, Yundong M, Qianhong C. A global maximumpower point tracking method based on interval short-circuit current. *In: 16th European conference on power electronics and applications (EPE'14-ECCE Europe)*, Lappeenranta, Finland, 26–28 August 2014. p. 1–8.

[6] El-Khatib, M. F., Sabry, M. N., Abu El-Sebah, M. I., & Maged, S. A. (2022). Experimental Modeling of a New Multi-Degree-of-Freedom Fuzzy Controller Based Maximum Power Point Tracking from a Photovoltaic System. *Applied System Innovation*, *5*(6), 114.

[7] Afghoul H, Krim F, Chikouche D, Beddar A. Tracking the maximum power from a PV panels using of neuro-fuzzycontroller. *In: IEEE International symposium on industrial electronics (ISIE)*, Taipei, Taiwan, 28–31 May 2013. p. 1–6.

[8] Mohamed A, Berzoy A, Mohammed O. Design and hardware implementation of FL-MPPT control of PV systems based on GA and small-signal analysis. *IEEE Transactions on Sustainable Energy*, Vol. 8, Issue: 1, January 2017, pp. 279-290.

[9] Eissa, Aly M.; ATIA, Mostafa R.; ROMAN, Magdy R. An effective programming by demonstration method for SMEs' industrial robots. *Journal of Machine Engineering*, 2020, 20.

[10] Andrea P, Andres C. Sliding-mode controller for maximum power point tracking in grid-connected photovoltaic systems. *Energies*, 2015, 8(11), 12363-12387.

[11] Pradhan R, Subudhi B. Double integral sliding mode MPPT control of a photovoltaic system. *IEEE Trans Control Syst Technol*., 2016;24(1):285–92.

[12] Montoya DG, Andres C, Giral R. Improved design of sliding mode controllers based on the requirements of MPPT techniques. *IEEE Trans Power Electron*., 2015:235–47.

[13] Sowparnika GC, Sivalingam A, Thirumarimurugan M. Design and implementation of sliding mode control for boost converter using PV cell. *Int Res J Emerg Trends Multidiscip (IRJETM)*, 2015;1(10):75–8.

[14] Prabhakaran A, Mathew AS. Sliding mode MPPT based control for a solar photovoltaic system. *Int Res J Eng Technol (IRJET)*, 2016;3(6):2600–4.

[15] Tamrakar V, Gupta SC, Sawle Y. Study of characteristics of single and double diode electrical equivalent circuit models of solar PV module. *In: International conference on energy systems and applications (ICESA)*, Pune, India, 30 Oct. – 1 Nov. 2015. p. 312–7.

[16] Lamnadi M, Trihi M, Bossoufi B, Boulezhar A. Comparative study of Ic, P&O and FLC method of MPPT algorithm for grid connected PV module. *J Theor Appl Inform Technol (JATIT)*, 2016;89(1):242–53.

[17] Bartoszewicz A, Z_uk J. Sliding mode control – basic concepts and current trends. *In: IEEE International Symposium on Industrial Electronics (ISIE)*, Bari, Italy, 4-7 July 2010. p. 3772–7.

[18] Meng Z, Shao W, Tang J, Zhou H. Sliding-mode control based on index control law for MPPT in photovoltaic systems. *IEEE Trans Electr Mach Syst*., 2018;2 (3):303–11.

[19] NagarajaRao S, Ashok Kumar D, SaiBabu Ch. PWM control strategies for multilevel inverters based on carrier redistribution technique. *Int J Electr Eng Technol (IJEET)*, 2014;5(8): 119–131.

[20] EL-FAKHARANY, A. E.; ATIA, M. R.; EL-SEBAH, MI Abu. Fuzzy Controller Algorithm for 3D Printer Heaters. *Journal of Advanced Research in Applied Mechanics*, 2017, 39.1.

[21] Mutoh N, Ohno M, Inoue T. A method for MPPT control while searching for parameters corresponding to weather conditions for PV generation systems. *Indus Elect IEEE Transact*., 2006;53:1055–65.

[22] Das P. Maximum power tracking based open circuit voltage method for PV system. *In: International Conference on Advances in Energy Research (ICAER)*, Mumbai, India, 15–17 December 2015 published by Elsevier. p. 2–13.

[23] Elgendy MA, Zahawi B, Atkinson DJ. ``Assessment of the incremental conductance maximum power point tracking algorithm. *IEEE Trans Sustain Energy*, 2013;4(1):108–17.

[24] Pradhan R, Subudhi B. Double integral sliding mode MPPT control of a photovoltaic system.

IEEE Trans Control Syst Technol., 2016;24(1):285–92.

[25] Meng Z, Shao W, Tang J, Zhou H. Sliding-mode control based on index control law for MPPT in photovoltaic systems. *IEEE Trans Electr Mach Syst*., 2018;2 (3):303–11.

[26] Mostafa, M. R., Saad, N. H., & El-sattar, A. A. (2020). Tracking the maximum power point of PV array by sliding mode control method. *Ain Shams Engineering Journal*, 11(1), 119-131.

[27] Amirnaser Yazdani, A Control Methodology and Characterization of Dynamics for a Photovoltaic (PV) System Interfaced With a Distribution Network, *IEEE Transactions On Power Delivery*, Vol. 24, N°. 3, July 2009, pp: 1538-1551.

[28] V. Salas, E. Olias, A. Barrado, A. Lazaro, Review of the Maximum Power Point Tracking Algorithms for Stand-Alone Photovoltaic Systems, *Solar Energy Materials & Solar Cells*, vol: 90, N°: 11, pp: 1555 –1578, 2006.

[29] Rekioua, D., Achour, A. Y., & Rekioua, T. (2013). Tracking power photovoltaic system with sliding mode control strategy. *Energy Procedia*, 36, 219-230.

[30] Zaid, S.A.; Albalawi, H.; Alatawi, K.S.; El-Rab, H.W.; El-Shimy, M.E.; Lakhouit, A.; Alhmiedat, T.A.; Kassem, A.M. Novel Fuzzy Controller for a Standalone Electric Vehicle Charging Station Supplied by Photovoltaic Energy. *Appl. Syst. Innov.* 2021, 4, 63.

[31] Tang, L.;Wang, X.; Xu,W.; Mu, C.; Zhao, B. Maximum power point tracking strategy for photovoltaic system based on fuzzy information diffusion under partial shading conditions. *Sol. Energy*, 2021, 220, 523–534.

[32] Zouirech, S., El Ougli, A., & Tidhaf, B. (2022). Implementation and Validation of Maximum Power Point Tracking (MPPT) of the Photovoltaic System on Arduino Microcontroller. *WSEAS Transactions on Systems and Control*, *17*, 418-427 https://doi.org/10.37394/23203.2022.17.46.

[33] W. I. Breesam, Real- time implementation of MPPT for renewable energy systems based on Artificial intelligence, *International Transactions on Electrical Energy Systems*, 2021, p. e12864.

[34] F. Mhamed, E. Mohamed Larbi, and Z. Smail, Hardware implementation of the fuzzy logic MPPT in an Arduino card using a Simulink support package for PV application, *IET Renewable Power Generation*, vol. 13, 2019, p. 10-518.

[35] K. Roshan, N. Geetha, and A. Dalvi, Comparative Study And Implementation Of Incremental Conductance Method And Perturb And Observe Method With Buck Converter By Using Arduino, *International Journal of Research in Engineering and Technology*, vol. 3, 2014, p. 461- 469.

[36] El-Sebah, M. I. A. (2016). Simplified intelligent Universal PID Controller. *International Journal of Engineering Research*, 5(1), 11-15.

[37] J. L. Santos, F. Antunes, A. Chehab, and C. Cruz, A maximum power point tracker for PV systems using a high performance boost converter, *Solar Energy*, vol. 80, 2006, p. 772-778.

[38] Saoud, M. S., Abbassi, H. A., Kermiche, S., & Nada, D. (2014). Improved incremental conductance method for maximum power point tracking using cuk converter. *MJMS Conference*, 1, 057-065.

[39] P.Ashish, "High-performance algorithms for drift avoidance and fast tracking in solar MPPT system", *IEEE Trans. on energy conversion*, vol. 23, no.2, pp.681– 689, June 2008.

[40] Salam Z, Kashif I, and Taheri H , "An Improved Two-Diode Photovoltaic (PV) Model for PV System" IEEE 2010. Kashif I, Salam Z "A review of maximum power point tracking techniques of PV system for uniform insolation and partial shading condition" *Renewable and Sustainable Energy Reviews*, 19 (2013) 475–48A.

[41] Ahmed. M. Kassem "Modeling, Analysis and Neural MPPT Control Design of a PV Generator Powered DC Motor-Pump System" *WSEAS Transactions on Systems*, Issue 12, Volume 10, December 2011, pp. 1109-2777.

[42] Othman, A. M., El-Arini, M. M., Fathy, A., & City, Z. (2014). Real world Maximum Power Point Tracking Based on Fuzzy Logic Control. *WSEAS Transactions on Power Systems*, 9, 232-241.

[43] EISSA, A., El-Khatib, M. F., & El-Sebah, M. I. A. (2023). Dynamics Analysis and Control of a Two-Link Manipulator. *WSEAS Transactions on Systems and Control*, 18, 487-497 https://doi.org/10.37394/23203.2023.18.52.

[44] L. Zhang, A. Al-Amoudi, and Y. Bai, "Realtime maximum power point tracking for gridconnected photovoltaic systems," in *Proc. Eighth Int. Conf. Power Electronics Variable Speed Drives*, , 2000, pp. 124-129.

[45] El-Khatib, M. F., & Maged, S. A. (2021, May). Low level position control for 4-DOF arm robot using fuzzy logic controller and 2-DOF PID controller. *In 2021 International Mobile, Intelligent, and Ubiquitous Computing Conference (MIUCC)*, pp. 258-262. IEEE.

[46] N. Femia, G. Petrone, G. Spagnuolo, and M. Vitelli, "Optimization of Perturb and Observe Maximum Power Point Tracking Method," *IEEE Trans. Power Electron.*, Vol. 20, , Jul. 2005, pp. 963-973.

[47] A. Brambilla, M. Gambarara, A. Garutti, and F. Ronchi, "New approach to photovoltaic arrays maximum power point tracking," in *30th Annual IEEE Power Electron. Specialists Conf.*, 1999, pp. 632-637.

[48] Gilbert M. Masters, *Renewable and Efficient Electric Power Systems*, John Wiley & Sons, Inc., Hoboken, New Jersey, 2004.

[49] Hohm, D. P. & M. E. Ropp, Comparative Study of Maximum Power Point Tracking Algorithms, *Progress in Photovoltaics: Research and Applications*, November 2002, pp. 47-62.

[50] C. Liu, B. Wu and R. Cheung, Advanced algorithm for MPPT control of photovoltaic systems, *Canadian Solar Buildings Conference Montreal*, August 20-24, 2004.

[51] Mayssa Farhat and Lassâad Sbita, Advanced fuzzy MPPT control algorithm for photovoltaic systems, *Science Academy Transactions on Renewable Energy Systems Engineering and Technology*, Vol. 1, No. 1, March 2011.

[52] Quamruzzaman, M., & Rahman, K. M. (2014). A modified perturb and observe maximum power point tracking technique for single-stage grid-connected photovoltaic inverter. *WSEAS Transactions on Power Systems*, 9, 111-118.

[53] T. Esram and P. L. Chapman, "Comparison of photovoltaic array maximum power point tracking techniques," *IEEE Trans. Energy Conv.*, Vol. 22, No. 2, , June 2007, pp. 439-449.

Contribution of Individual Authors to the Creation of a Scientific Article (Ghostwriting Policy)

The authors equally contributed in the present research, at all stages from the formulation of the problem to the final findings and solution.

Sources of Funding for Research Presented in a Scientific Article or Scientific Article Itself

No funding was received for conducting this study.

Conflict of Interest

The authors have no conflicts of interest to declare.